applied sciences

MDPI

Article

Chestnut Burr as a Multifunctional Filler for PLA-Based Bio-Composites: Processing, Characterization, and Antioxidant Functionality

Tommaso Olmastroni [1,†], Simone Pepi [1,†], Milad Sarwari [1], Eugenio Paccagnini [2], Alfonso Trezza [1,*], Anna Visibelli [1], Pietro Lupetti [2], Agnese Magnani [1], Valter Travagli [1], Michela Geminiani [1,3,*] and Annalisa Santucci [1,3,4]

[1] Department of Biotechnology, Chemistry and Pharmacy, University of Siena, Via A. Moro 2, 53100 Siena, Italy; tommaso.olmastroni@student.unisi.it (T.O.); simone.pepi@unisi.it (S.P.); m.sarwari@student.unisi.it (M.S.); anna.visibelli2@unisi.it (A.V.); agnese.magnani@unisi.it (A.M.); valter.travagli@unisi.it (V.T.); annalisa.santucci@unisi.it (A.S.)
[2] Department of Life Sciences, University of Siena, Via A. Moro 2, 53100 Siena, Italy; eugenio.paccagnini@unisi.it (E.P.); pietro.lupetti@unisi.it (P.L.)
[3] SienabioACTIVE, Via A. Moro 2, 53100 Siena, Italy
[4] ARTES 4.0, Viale Rinaldo Piaggio 34, 56025 Pontedera, Italy
* Correspondence: alfonso.trezza2@unisi.it (A.T.); michela.geminiani@unisi.it (M.G.)
† These authors contributed equally to this work.

Abstract

This study explores the valorization of chestnut burrs (*Castanea sativa*), an abundant agro-industrial residue, as a natural filler for polylactic acid (PLA)-based biocomposites with potential applications in additive manufacturing. PLA/chestnut burr composite filaments were prepared by melt extrusion with filler contents of 2.5%, 5%, 10%, and 15% *w*/*w*, and their chemical, thermal, morphological, and mechanical properties were systematically characterized. ATR-FTIR confirmed the absence of major chemical modifications of the PLA matrix. Thermogravimetric analysis (TGA) and differential scanning calorimetry (DSC), the latter performed on both the extruded filaments and the material after fused deposition modeling (FDM) 3D printing, revealed a slight decrease in thermal stability with increasing filler content, coupled with enhanced crystallinity. Mechanical properties analysis showed that the addition of chestnut burrs did not negatively impact the viscoelastic behavior of the filaments. Scanning electron microscopy (SEM) highlighted good filler dispersion up to 5% loading, while higher percentages led to increased surface roughness and microvoids. Importantly, antioxidant activity assays (DPPH, ABTS, FRAP, and Folin–Ciocâlteu) demonstrated that the incorporation of chestnut burr significantly enhanced the radical-scavenging capacity, reducing power, and total phenolic content (TPC) of PLA. These functionalities were preserved, and in some cases amplified, after FDM 3D printing, indicating that the processing conditions did not degrade the bioactive constituents. Overall, chestnut burrs are confirmed as an effective multifunctional filler for PLA, improving its antioxidant activity while maintaining structural and thermal performance, supporting the development of sustainable biocomposites for emerging applications.

Keywords: chestnut burr; PLA; biocomposite; 3D printing; antioxidant activity; thermal properties; mechanical properties; morphological properties; natural fillers

check for updates

Academic Editors: Antonios E. Koutelidakis, Ena Cegledi and Ana Dobrinčić

Received: 29 September 2025
Revised: 27 October 2025
Accepted: 29 October 2025
Published: 4 November 2025

Citation: Olmastroni, T.; Pepi, S.; Sarwari, M.; Paccagnini, E.; Trezza, A.; Visibelli, A.; Lupetti, P.; Magnani, A.; Travagli, V.; Geminiani, M.; et al. Chestnut Burr as a Multifunctional Filler for PLA-Based Bio-Composites: Processing, Characterization, and Antioxidant Functionality. *Appl. Sci.* **2025**, *15*, 11743. https://doi.org/10.3390/app152111743

Copyright: © 2025 by the authors. Licensee MDPI, Basel, Switzerland. This article is an open access article distributed under the terms and conditions of the Creative Commons Attribution (CC BY) license (https://creativecommons.org/licenses/by/4.0/).

1. Introduction

The enormous global production of plastic has raised growing concerns about environmental pollution caused by plastic waste. One of the most promising approaches is to replace fossil-based plastics with biodegradable bioplastics [1].

Polylactic acid (PLA) has emerged as one of the most widely used bioplastics because it is derived from renewable resources (such as corn starch) and has excellent mechanical and chemical properties, allowing it to be used in a variety of industries including packaging, agriculture, and biomedicine. However, PLA has some inherent limitations, including low heat resistance and fragility, making it less durable than traditional plastics. These constraints limit the potential applications of PLA in various areas; efforts are being made to improve the mechanical and thermal properties of PLA so that it can be a better alternative to traditional polymers [2].

To overcome these drawbacks and broaden the applications of PLA, numerous studies have investigated adding additives or reinforcements to the polymer. In particular, incorporating natural fibers or fillers derived from agro-industrial waste into PLA has proven to be an effective strategy for improving some of the material's properties while maintaining its overall biodegradability [3].

The use of bio-based fillers not only may improve the stiffness, strength, and thermal stability of the composite, but also aligns with the circular bioeconomy principle, which maximizes the use of biomass residues while reducing waste through their conversion into new resources [4].

Numerous agricultural by-products have been studied as reinforcements for PLA-based biocomposites, including different lignocellulosic wastes. For example, it has been observed that various fillers from plant waste can enhance certain properties of PLA biocomposites (such as the elastic modulus), although the extent and nature of the improvement depend on the type of filler and its percentage content. Generally, composites with acceptable mechanical and thermal properties are a suitable replacement for non-biodegradable petroleum-based products [5].

The chestnut burr, among other usable agro-industrial wastes, emerges as a potential resource. It is an abundant and currently undervalued lignocellulosic residue. Following the harvest of chestnuts, the burr is discarded and usually burned, emitting CO_2 and contributing to global warming. The chestnut burr, in addition to its well-known antioxidant, anti-inflammatory, and antimicrobial properties, is also recognized for its composition of lignin and cellulose, making it a promising candidate for potential use as a natural filler in bio-based materials [6–8].

Beyond enhancing the sustainability of polymeric materials, the current development of PLA-based biocomposites is also driven by the growing interest in active and functional packaging systems. These materials are designed to go beyond the traditional passive barrier function by providing additional protective roles, such as antioxidant and antimicrobial properties, thereby contributing to the quality and stability of packaged products. Several studies have shown that the incorporation of natural fillers can effectively impart antioxidant and functional properties to PLA-based systems, enabling the design of fully bio-based and compostable active packaging materials [9,10]. Within this framework, the chestnut burr, rich in phenolic compounds and lignocellulosic components, is a promising additive capable of improving both the renewable content and the functional performance of PLA composites.

Moreover, additive manufacturing provides a powerful platform for producing customized and functional components from a wide range of materials. In this context, several studies have demonstrated the suitability of PLA-based biocomposites containing natural fillers for use in Fused Deposition Modeling (FDM), highlighting their good printabil-

ity and sustainable performance [11]. Furthermore, advances in additive manufacturing technologies have enabled the design and optimization of individualized structures for biomedical applications [12], supporting the potential of the developed PLA/chestnut burr composite for future advanced manufacturing applications.

Several studies recently have used plant fibers or agro-industrial waste as a natural filler to strengthen biodegradable polymer matrices like PLA. It has been demonstrated that natural fibers can be integrated into PLA, yielding positive results in terms of the bio-composite's mechanical and chemical properties. Alothman et al. developed PLA biocomposites from natural fibers and demonstrated that they are suitable for various applications due to their high stiffness, tensile strength, and dimensional stability [13]. In another study, rapeseed straw was evaluated as a sustainable filler material in PLA based biocomposites. The study examined thermal, morphological, mechanical, and physical properties, and found promising results, such as increased stiffness of PLA with increased rapeseed straw loading [14].

By integrating chestnut burr, a lignocellulosic agricultural residue, into a PLA matrix, the primary goal of this study is to create and describe a novel bio-based composite material.

Accordingly, PLA-based biocomposites were prepared by hot-melt extrusion with varying filler contents (2.5%, 5%, 10%, and 15% by weight). Both the PLA matrix and the chestnut burr filler are entirely derived from renewable resources. Therefore, the resulting composites are fully biobased. The incorporation of the chestnut burr contributes to the fraction of waste-derived renewable content, thus enhancing the circularity and sustainability of the developed material. This was done to value agro-industrial waste in line with the circular bioeconomy's fundamental principles. To determine how the addition of chestnut burr affected the chemical, thermal, and mechanical properties of PLA, the resultant composite filaments were carefully characterised. The molecular structure and potential chemical interactions were investigated using FT-IR spectroscopy; thermal stability was assessed using thermogravimetric analysis (TGA); and glass transition, cold crystallisation, melting behaviour, and general crystallinity were studied using differential scanning calorimetry (DSC). The mechanical response of the materials was further examined. Although the focus of the study is on material development and characterization, the extruded filaments were also processed through Fused Deposition Modelling (FDM) 3D printing using standard PLA conditions. This step was introduced to explore potential practical applications and to assess the thermal behavior of the biocomposite material after the printing process through DSC analysis. Importantly, because chestnut burr is a known source of phenolic compounds, the study also investigates the antioxidant functionality imparted by the filler. The radical scavenging activity, reducing power, and total phenolic content (TPC) of the composites, before and after 3D printing, were quantified by DPPH, ABTS/TEAC, FRAP, and Folin–Ciocâlteu assays. Overall, this work aims to demonstrate the feasibility of producing PLA-based biocomposites containing a natural lignocellulosic filler that improves or at least maintains the performance of neat PLA while introducing stable antioxidant activity, thereby supporting the use of agricultural residues in sustainable materials for emerging applications such as active packaging.

2. Materials and Methods

2.1. Raw Materials and Filler Preparation

The chestnut burrs were collected in Monte Amiata, Tuscany, a key area for chestnut production in Italy. They were manually selected, and impurities were removed before being air-dried until they reached a constant weight. They were then mechanically ground with a high-speed laboratory blender (Microtron MB 550, Kinematica AG, Lucerne, Switzerland) until a roughly uniform powder was produced. The powder was then sifted through

a 200 µm mesh size sieve to ensure consistent particle size distribution and uniform dispersion in the polymer during the extrusion process. To prevent moisture absorption, the powder was stored in a dryer at 40 °C until it was mixed with PLA.

PLA pellets (NatureWorks Ingeo™ 4043D, NatureWorks LLC, Minnetonka, MN, USA) were dried in an air oven at 60 °C for 12 h and transferred immediately after drying to a sealed container with desiccant.

2.2. Composite Filament Fabrication

PLA/chestnut burr filaments were manufactured using a Felfil Evo Filament Extruder (Felfil S.r.l., Turin, Italy). Five formulations were prepared: pure PLA (PLA100) and PLA containing 2.5% (PLA97.5), 5% (PLA95), 10% (PLA90), and 15% (PLA85) by weight of chestnut burr. The mixtures were obtained by manually mixing biomass powder with PLA pellets until the filler was evenly distributed.

The extrusion was performed at 180 °C (±10) and 5 rpm, the gold standard for PLA, according to the Felfill Evo Filament Extruder manual, with a 1.75 mm nozzle diameter. To ensure the quality of the final product, the first centimeters of extruded filament were discarded to stabilize the process. To improve homogeneity, the filament produced from the first extrusion was firstly shredded with Felfil Shredder (Felfil S.r.l., Turin, Italy), and subsequently re-extruded.

The extruded filament was immediately wound with a Felfil Spooler system (Felfil S.r.l., Turin, Italy), allowing tension and diameter to be controlled precisely. The target filament diameter was set at 1.75 mm.

2.3. Three-Dimensional Printing Conditions

Selected formulations were printed using a Prusa i3 MK3S+ fused deposition modelling (FDM) 3D printer (Prusa Research, Prague, Czech Republic) to assess the printability of the created biocomposite filaments and their behaviour following processing, specifically to evaluate the thermal behavior with DSC and to assess antioxidant power through spectrophotometric assays. Filament diameter was set to 1.75 mm, and a 0.4 mm brass nozzle was used. To guarantee ideal adhesion throughout the printing process, the bed temperature was set at 60 °C and the extrusion temperature was kept at 210 °C. In order to account for the minor variations in flow behaviour seen in the composite filaments, these parameters were chosen based on standard PLA printing settings.

2.4. Mechanical Properties

The mechanical properties (complex modulus, tangent of phase angle, and stiffness) in the linear viscoelastic region, as well as their temperature dependency, were tested using an AR2000ex rheometer (TA Instruments, New Castle, DE, USA), equipped with an Environmental Test Chamber (ETC) and using a double clamp geometry. Rheology Advantage Instrument Control (v. 5.8.2) and Rheology Advantage Data Analysis (v. 5.7.0) were used for instrument control and for data analysis, respectively. The test to evaluate the linear viscoelastic region (LVR) was performed from 10^{-2}% to 10%, at a constant frequency of 1 Hz, at 25 °C. The mechanical parameters were evaluated using two different tests:

- Frequency sweep, using a 0.1% constant strain (selected within the LVR), in a frequency range from 0.1 Hz to 10 Hz, at 25 °C;
- Temperature sweep, at constant strain and frequency, 0.1% and 1 Hz, respectively, sweeping the temperature from 30 °C to 80 °C, at a heating rate of 10 °C/min.

2.5. Infrared Spectroscopy (ATR FT-IR)

The FT-IR analysis was performed on dry filaments at room temperature, within the spectral range 700–4000 cm^{-1}, averaging 64 scans at a spectral resolution of 4 cm^{-1}, using a Nicolet iS50 (Thermo Scientific, Waltham, MA, USA) instrument, equipped with an ATR (Attenuated Total Reflection) cell with Ge crystal as internal reflection element.

2.6. Thermogravimetric Analysis (TGA)

The TGA analysis was performed using a SDT-Q600 (TA Instruments), and Thermal Advantage (rel. 5.5.22) and TA Instruments Universal Analysis 2000 (ver. 4.5.4) software were, respectively, used for instrument control and data analysis. 10 mg–20 mg of the dry filament and chestnut were put in a Pt crucible and heated from 30 °C to 450 °C at a heating rate of 10 °C/min, in a nitrogen atmosphere (100 mL/min).

2.7. Differential Scanning Calorimetry (DSC)

The DSC analyses were performed using a DSC 2500 (TA Instruments, New Castle, DE, USA) and the TRIOS (v. 5.7.0.56, TA Instruments-Waters LLC, New Castle, DE, USA) software for both the instrument control and data analysis. 1–5 mg of the dry filament were hermetically sealed in a hermetic aluminum pan, using an empty one as reference. The samples were heated up from 45 °C to 200 °C at a heating rate of 1 °C/min., and the cell was purged with 50 mL/min. of nitrogen [15].

2.8. Scanning Electronic Microscope (SEM)

Morphological analyses were performed using a Quanta 400 Environmental Scanning Electron Microscope (ESEM, FEI, ESEM, FEI Company, Hillsboro, OR, USA). Samples were mounted directly onto aluminum stubs and coated with a 20 nm layer of gold/palladium alloy (60/40) using a MED 010 sputter coater (Balzers Union AG, Balzers, Liechtenstein). The amount of sample varied depending on the filament, but this did not affect the quality of the observations. All images were acquired under high vacuum conditions.

2.9. Antioxidant Analysis of Composite Filaments Pre- and Post-Printing

The antioxidant activity of the PLA-based composite filament at the highest filler concentration, both before (PLA85) and after 3D printing (PLA85 post printing), was evaluated using spectrophotometric assays. Pure PLA (PLA100) was used as the negative control. Extracts were prepared and analyzed using FRAP, DPPH, ABTS, and Folin–Ciocâlteu methods as described below. For all the assays, data are presented as mean ± SD (n = 3). Group differences (PLA100, PLA85, and PLA85 post printing) were tested by one-way ANOVA followed by Dunnett's multiple comparison test to compare each treatment with PLA100 (a p-value < 0.05 was considered significant). Analyses were performed using GraphPad Prism 9.0 (GraphPad Software, San Diego, CA, USA).

2.9.1. Extraction of Antioxidant Compounds

Filaments based on PLA and chestnut burr at the highest concentration (15%), both before and after 3D printing, were manually cut into fragments (<5 mm) using laboratory scissors. For each sample, 200 mg of material were weighed into 15 mL Falcon tubes and extracted with 4 mL of a 70:30 ethanol–water solution. Samples were sonicated with an immersed probe (20 kHz) for 30 min, then centrifuged at 4000 rpm for 10 min. The supernatants were carefully collected and stored at 4 °C in the dark until further analysis [16].

2.9.2. Total Phenolic Content (TPC)

TPC was determined using the Folin–Ciocâlteu colorimetric assay, adapted to 96-well microplate format [17]. For each well, 20 µL of extract were mixed with 100 µL of 1 N

Folin–Ciocâlteu reagent, followed by a 5-min incubation at room temperature. Then, 80 µL of saturated Na_2CO_3 solution were added. Plates were incubated for 90 min in the dark at room temperature, and absorbance was measured at 725 nm using an EnVision system, software v.1.13 (PerkinElmer Inc., Waltham, MA, USA). A blank solution containing all reagents except for the extract, was also prepared. A calibration curve was constructed using gallic acid standards (20–120 µg/mL). Results were expressed as mg gallic acid equivalents per gram of filament (mg GAE/g).

2.9.3. Determination of Reducing Power

The antioxidant capacity of the extracts was evaluated using the ferric-reducing antioxidant power (FRAP) assay adapted to 96-well microplate format [18]. For each well, 20 µL of sample or ascorbic acid standard were mixed with 100 µL of 0.2 M phosphate buffer (pH 6.6) and 100 µL of 1% potassium ferricyanide ($K_3[Fe(CN)_6]$). The plate was incubated at 50 °C for 20 min. After incubation, 100 µL of 10% trichloroacetic acid (TCA) were added, followed by a short resting period of 5–10 min at room temperature. Subsequently, 250 µL of distilled water and 50 µL of 0.1% ferric chloride ($FeCl_3$) were added to each well. The formation of the blue-green Fe^{2+} complex was measured by reading the absorbance at 700 nm. A calibration curve was obtained using ascorbic acid in the range of 20–120 µg/mL, and results were expressed as mg AAE per gram of filament (mg AAE/g).

2.9.4. DPPH Free-Radical Scavenging Activity

The 2,2-diphenyl-1-picrylhydrazyl (DPPH) free-radical scavenging activity was determined by mixing 100 µL of extract with 100 µL of a 0.1 mM DPPH solution prepared in ethanol. The mixtures were incubated in the dark at 37 °C for 30 min. After incubation, the absorbance was measured at 517 nm [19]. Trolox was used as the standard to generate the calibration curve. Results were expressed both as Trolox Equivalent Antioxidant Capacity (TEAC, mg TE/g of sample), and as radical scavenging activity (RSA%).

2.9.5. ABTS+ Free-Radical Scavenging Activity

The antioxidant capacity based on 2,2′-azino-bis(3-ethylbenzothiazoline-6-sulfonic acid) ($ABTS^+$) radical cation reduction was evaluated using the OxiSelect™ TEAC Assay Kit (Cell Biolabs Inc., San Diego, CA, USA), following the manufacturer's instruction. Briefly, 25 µL of each sample, at different concentrations, were added to 150 µL of freshly diluted $ABTS^+$ working solution (1:50 dilution) in a 96-well microplate. The plate was gently shaken for 5 min, and absorbance was then measured at 405 nm. Antioxidant activity was quantified and expressed as milligrams of Trolox equivalents (mg TE) per gram of sample and as radical scavenging activity (RSA%).

3. Results

3.1. Infrared Spectroscopy (ATR FT-IR)

Infrared analysis was performed to investigate the chemical composition of the materials. All spectra possess the same bands, as shown in Figure 1. Concerning the main bands observed in the spectra, the 1752 cm^{-1} absorption can be assigned to the -C=O stretching of the carboxyl group, the 1455 cm^{-1} absorption is assigned to the CH_3 bending, the 1382 cm^{-1} and 1362 cm^{-1} are assigned, respectively, to the symmetric and asymmetric CH bending, the 1366 cm^{-1} to the -C=O bending, the 1183 cm^{-1}, 1129 cm^{-1} and 1087 cm^{-1} to the -C-O- stretching, and the 1046 cm^{-1} to the -OH bending [20]. The infrared data suggested that, within the PLA-based filament, the chestnut burr does not produce any significant compositional change in the starting polymer, since all the observed bands are assigned to PLA polymer. This finding is consistent with previous studies on wood-

sawdust reinforced PLA where it was similarly observed that the natural filler does not chemically interact with the PLA matrix [21].

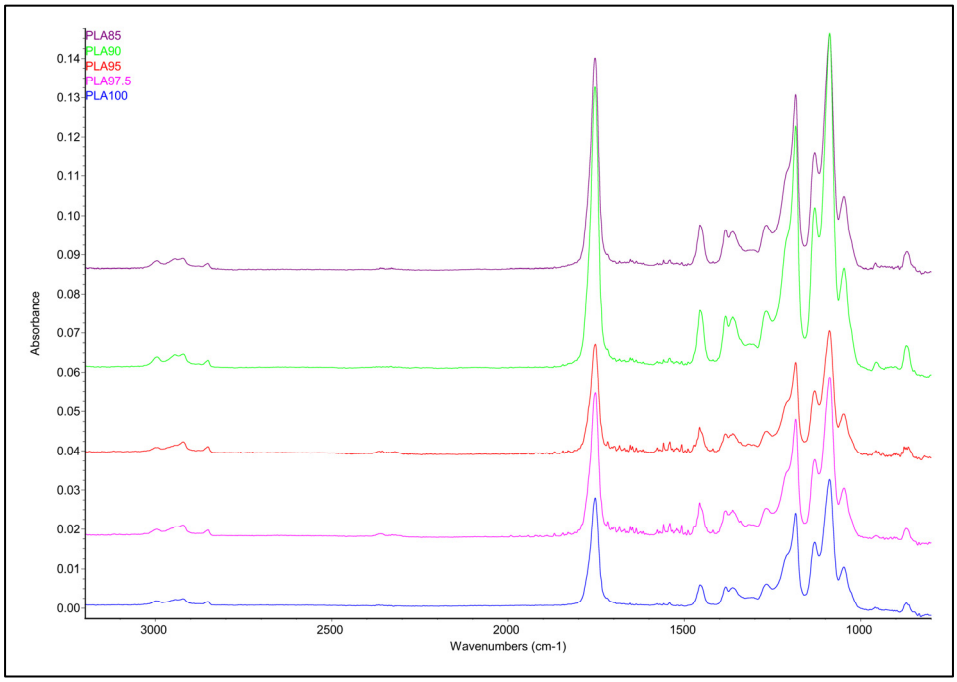

Figure 1. ATR FT-IR stacked spectra of the PLA-based filaments.

3.2. Thermogravimetric Analysis (TGA)

TGA was performed to test the thermal stability of the PLA-based materials. The TGA results are reported in Figure 2a and in Table 1. They are expressed in terms of weight loss percentages w/w, residue at 450 °C and T_{max} of the main degradation peak as determined by the first derivative with respect to temperature (DTG, %/°C) of thermograms.

The TGA data reveal that the weight loss from the first range of temperature (30–200 °C), which can be associated with the loss of the water and volatile molecules, is increased by about 50% for the PLA90 and PLA85. This behavior can be associated with the increased presence of chestnut burr in the filament, which results in an increased hydrophilicity of the material. The trend observed in the second temperature range (200–450 °C), corresponding to the degradation of the aliphatic chains and to the degradation of the whole polymer [22], shows a weight loss decrease according to the increase in the residue at 450 °C with increasing of the natural filler content. Figure 2 summarizes the results for the DTG of the PLA-based filaments. The thermograms show a common behavior of the chestnut burr containing PLA-based filaments: those materials possess a very similar value of T_{max} (331 °C ± 3 °C), and a similar slight decrease in thermal stability (−4.1%, with respect to the PLA100), reflected in the decreasing of the T_{max} of the main transition, as shown in the last column of Table 1. Thus, thermal characterization of the composite filaments confirms that their degradation onset temperature is well above typical processing ranges (e.g., >260 °C), in line with findings from recent studies. This wide processing window ensures that extrusion and FDM 3D printing, performed in a range of 180–220 °C, occur safely and without significant material thermal degradation [23].

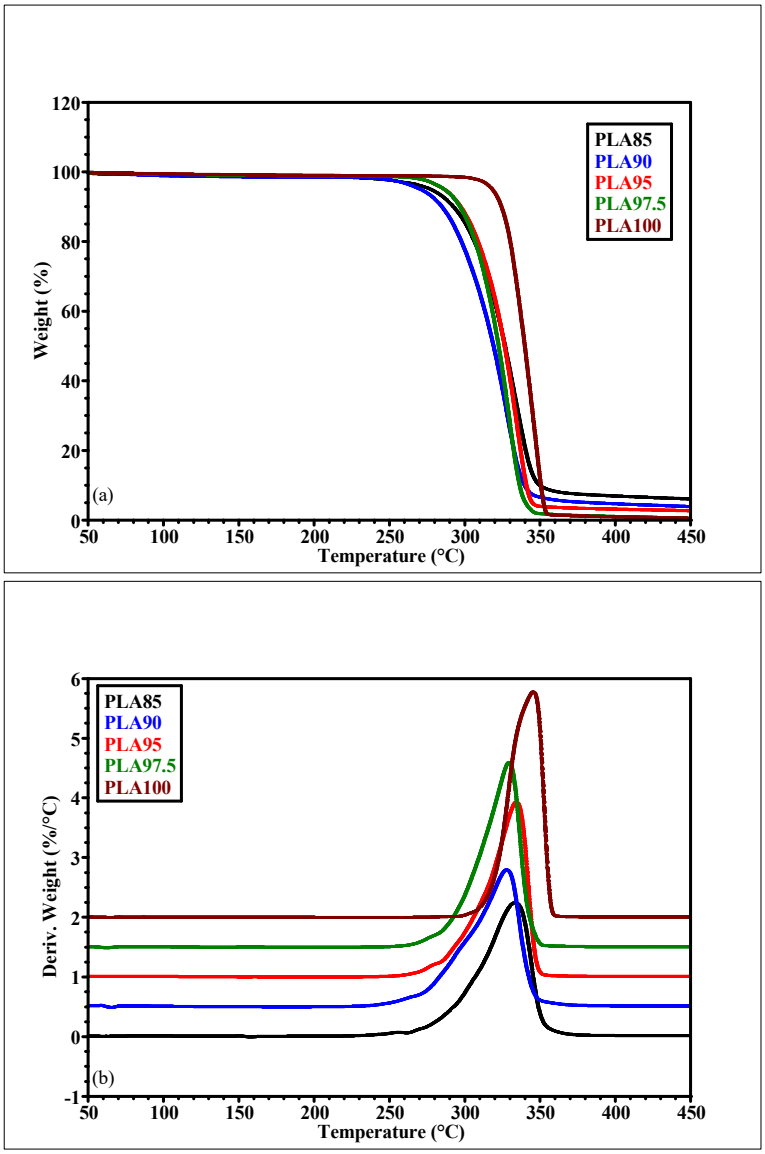

Figure 2. (**a**) TGA and (**b**) DTG thermogram of the five PLA-based filaments, deriving from the TGA analysis.

Table 1. TGA and DTG results of the PLA-based filament.

Sample	Weight Loss at 30–200 °C (% *w*/*w*)	Weight Loss at 200–450 °C (% *w*/*w*)	Residue at 450 °C (% *w*/*w*)	DTG Tmax (°C)
PLA100	1.0% ± 0.1%	98.5% ± 3.0%	0.5% ± 0.0%	345 °C ± 6 °C
PLA97.5	1.1% ± 0.1%	98.4% ± 2.0%	0.5% ± 0.0%	329 °C ± 2 °C
PLA95	1.0% ± 0.1%	96.3% ± 3.9%	2.7% ± 0.1%	334 °C ± 4 °C
PLA90	1.5% ± 0.0%	94.6% ± 4.7%	3.9% ± 0.1%	328 °C ± 4 °C
PLA85	1.4% ± 0.0%	92.6% ± 3.7%	6.1% ± 0.3%	333 °C ± 3 °C

3.3. Differential Scanning Calorimetry (DSC)

The DSC analysis was used to evaluate the thermal behavior of the PLA-based filaments after both extrusion and printing processes. PLA100 curves are depicted in Figure 3a for pre- and post-printing. From the thermograms some typical heat transitions of PLA are evident, i.e., glass transition (T_g), cold crystallization, and melting phenomena. As the

T_g (I) is concerned, the plot evidences a small endothermic peak in the pre-printing thermogram at the end of the transition. This transition may be assigned to the non-reversible enthalpy relaxation due to the thermal history of the filament production process. In the post-printing curve, the endothermic peak disappeared because of the printing process that removes all factors that generate that transition. The exothermic transition (II) is a cold crystallization process, followed by the endothermic melting ones (III and IV). The melting process shows two different peaks due to two different forms of the PLA crystals: the (III) peak may be associated with defective and not completely formed structures (α'-crystals), and the (IV) peak may be assigned to the properly and perfectly crystallized structures (α-crystals) [24]. Thus, in that case, the printing process does not remove or affect this defect in the crystallization phenomena of the PLA.

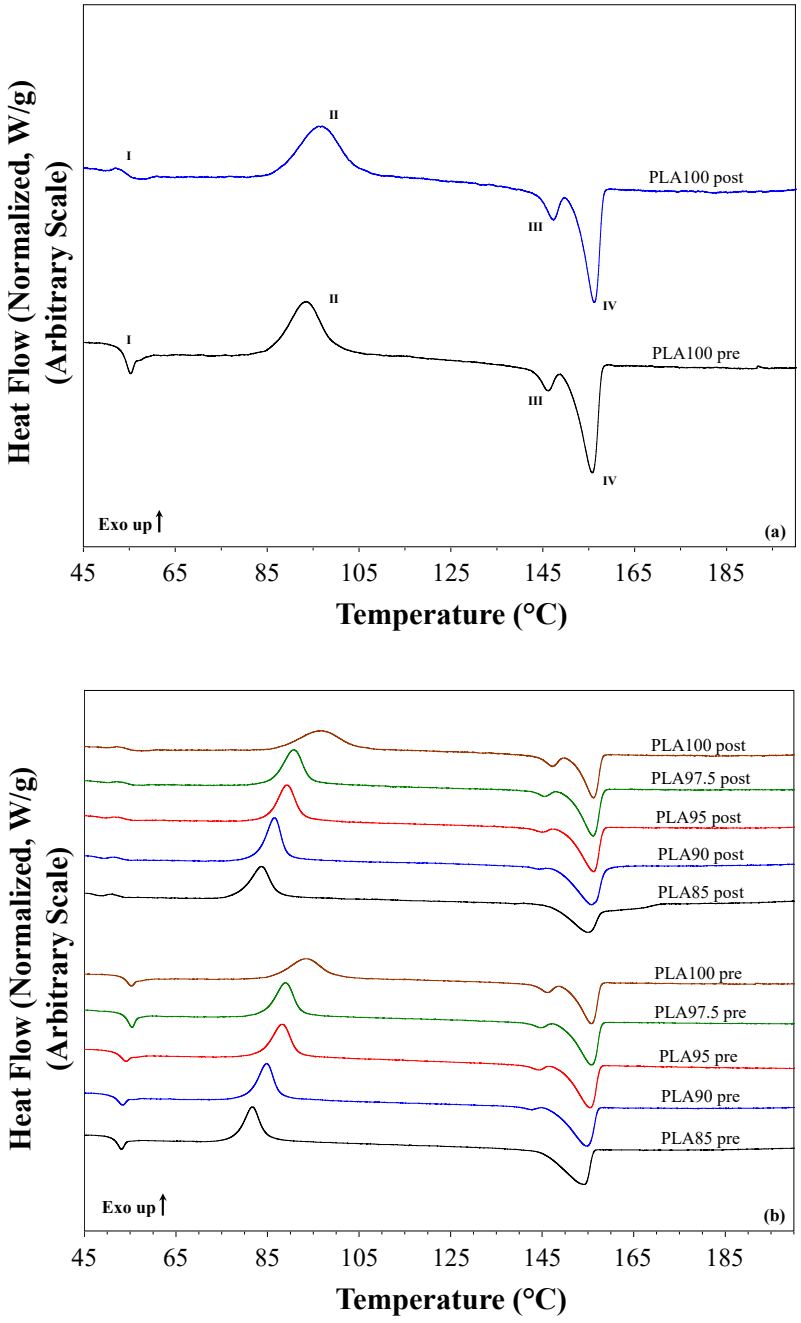

Figure 3. DSC thermograms of (**a**) PLA100 for the pre- and post-printing filaments with the highlights of the main thermal transitions of the PLA materials, and (**b**) all the pre- and post-printing filaments.

As regards to the thermograms of all the PLA-based filaments, some differences can be observed both within and between the two series of samples, as well as the effect of the chestnut burr incorporation on the thermal behavior of the material. The thermograms of pre-printing (bottom) and post-printing (upper) filaments are depicted in Figure 3b. The data evidenced that the amount of the filler in the filaments does not affect the T_g, and the printing process removes the small endothermic peak at the end of the glass transition for all the PLA filaments, without affecting the main transition process. This feature is confirmed by the data of Table 2, as the midpoint temperature of the T_g does not undergo any significant variations in all the two sample series. The cold crystallization appears to be affected only by the chestnut burr content in terms of temperature ($T_{cc,max}$), but not in the enthalpy of crystallization (ΔH_{cc}) (see Table 2). Figure 3b shows the effect of the filler on the filaments, reflected in a temperature drop of the exothermic transition maximum, which is strictly correlated with the chestnut burr content, with the same trend observed for the pre- and post-printing materials. As far as the melting behavior is concerned, the data suggested that both the melting temperature ($T_{m,max}$) and enthalpy of fusion (ΔH_m) do not change with the printing process, and no significant differences in the two parameters are observed after the material's printing. The amount of the α'-crystals decreases, increasing the chestnut burr content in the filament, and this kind of crystal disappears completely in the PLA85 pre- and post-printing. This aspect emphasizes the positive effect of the filler as it acts as a nucleation center favoring the formation of α-crystals while inhibiting that of α'-crystals. The crystallinity of the PLA in the filaments, with respect to 100% crystalline PLA is reported in Table 2. All the pre-printing filaments show almost the same crystallinity. The degree of crystallinity increased in the post-printing filaments compared to the corresponding pre-printing material, except for PLA97.5. This trend shows a direct correlation with the increasing chestnut burr content, suggesting that the presence of biomass promotes a higher degree of structural organization in the material. The preservation or slight enhancement of crystallinity after FDM printing suggests that the polymeric matrix remains thermally stable during processing, indirectly supporting the retention of the material's overall mechanical integrity.

Table 2. DSC results of the PLA-based filament in terms of Tg, ΔH of crystallization and melting, and crystallinity.

Sample	Tg (T, °C)	ΔHcc (J g^{-1})	ΔHm (J g^{-1})	Tcc,max (°C)	Tm,max (°C)	Crystallinity (%) (*)
PLA100 pre	54.5	22.61	28.68	81.7	154.2	30.8%
PLA97.5 pre	54.7	23.16	30.68	84.8	154.8	33.0%
PLA95 pre	53.2	23.80	30.08	88.3	155.4	32.3%
PLA90 pre	52.6	24.19	30.84	88.9	155.8	33.2%
PLA85 pre	52.5	23.79	32.70	93.6	155.8	35.2%
PLA100 post	54.2	22.61	30.00	83.7	154.9	32.3%
PLA97.5 post	54.9	23.16	30.45	86.5	155.8	32.7%
PLA95 post	53.7	23.80	31.73	89.2	156.3	34.1%
PLA90 post	53.1	24.19	35.39	90.8	156.1	38.1%
PLA85 post	52.5	23.79	34.58	96.8	156.3	37.2%

(*) Calculated in respect to the 100% crystalline PLA: 93 J g^{-1} [25].

3.4. Mechanical Properties

The mechanical properties were evaluated in terms of complex modulus (G*), tangent of phase angle (tan δ), and stiffness, within the linear viscoelastic region (LVR), and their temperature dependency was also studied. The results of the frequency sweep test for the mechanical properties (G*, tan δ, and stiffness) are shown in Figure 4.

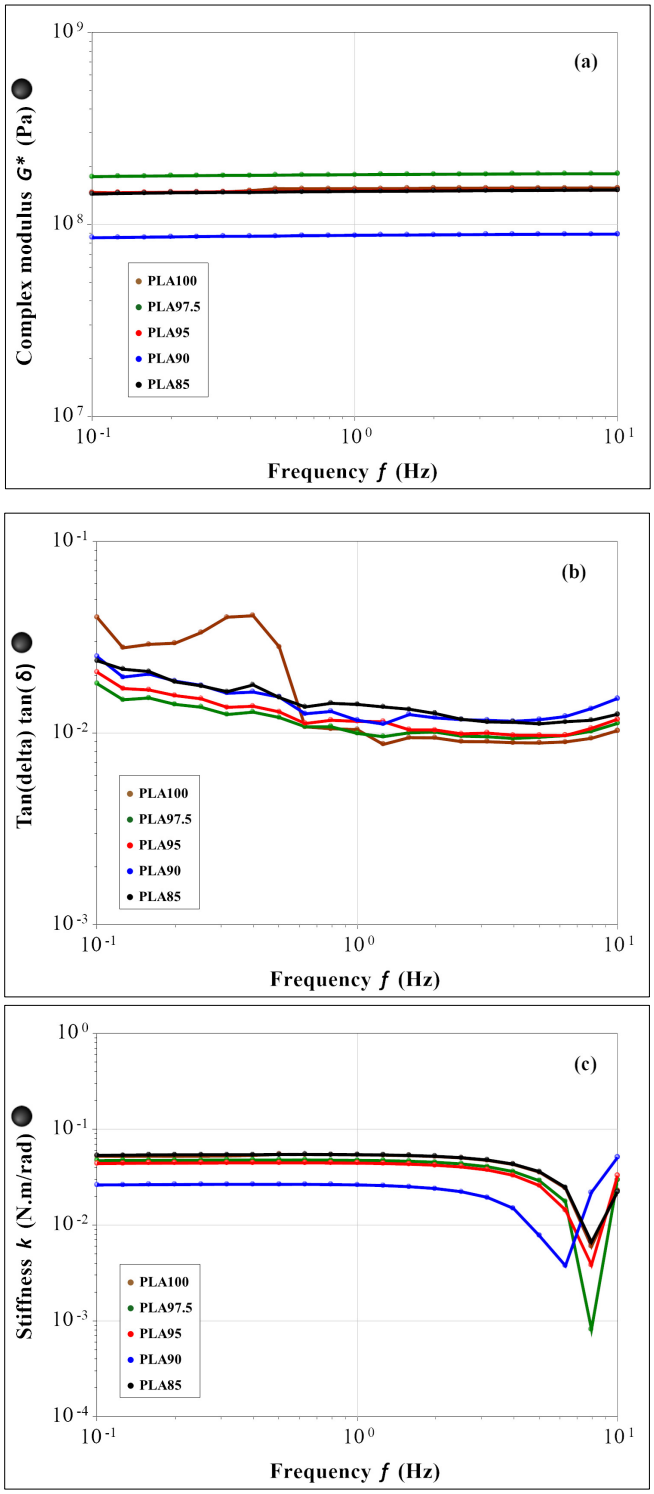

Figure 4. Frequency sweep results within the LVR for the (**a**) complex modulus, (**b**) tan δ and (**c**) stiffness; for PLA85 in black, PLA90 in blue, PLA95 in red, PLA 97.5 in green and PLA100 in brown.

Figure 4a summarizes the complex modulus data ($|G^*| = G' + iG''$) that indicates the overall mechanical properties of the material. All the samples show a constant behavior in the whole range of frequency, independently of the chestnut burr content. Figure 4b shows the data of tan δ, that corresponds to the ratio between the viscous and elastic moduli ($\tan \delta = G''/G'$). All the tested materials exhibit a constant value of this parameter in the whole frequency range. The same trend is observed for the stiffness parameter (Figure 4c).

The results of the temperature sweep test are reported in Figure 5 for G*, tan δ and the stiffness. As for the frequency sweep test, both the behavior of the materials and the magnitude of the evaluated parameters appear to be the same in the whole temperature range. Figure 5a shows a constant complex modulus till about 57 °C (T_g value of the PLA-based filaments) for all samples. The difference in the glass transition temperature found by this test, to that evaluated by DSC thermograms, is associated with the different heating rate used by the two techniques: 10 °C/min for the mechanical test and 1 °C/min. for the DSC one. The increase in T_g values using a higher heating rate is caused by the thermal inertia of the sample, which influences the temperature of the thermal phenomenon less by using a low heating rate. After the glass transition, the G* decreases coherently for all samples, of two orders of magnitude at 80 °C. From the overall data, it is possible to assess that the presence and the amount of the chestnut burr do not affect the mechanical properties and the mechanical behavior of the PLA-based materials. Moreover, SEM analysis, discussed in the following paragraph, confirmed that up to 5 wt% chestnut burr the morphology of the PLA matrix remains homogeneous and free from delamination or microvoids. This morphological stability, combined with the mechanical and thermal results, suggests that the incorporation of chestnut burr does not compromise the structural integrity of the material. Therefore, no evidence indicates that the composite filaments would experience any mechanical weakening after FDM printing. Additionally, the fabrication of printed specimens for DSC and antioxidant activity tests was successfully performed for all formulations without any nozzle clogging, confirming the good printability and processing reliability of the composite filaments. Even the formulations containing 10 wt% and 15 wt% chestnut burr were successfully printed despite the slightly higher surface roughness observed in SEM images.

3.5. Morphological Analysis

Morphological evaluation through SEM allowed a detailed observation of the microstructure of PLA/chestnut burr filaments at various filler concentrations (0–15%). Both surface and cross-sectional views were analyzed to visually assess filler dispersion, interfacial adhesion, and the presence of morphological features which could be relevant to the performance of the composite.

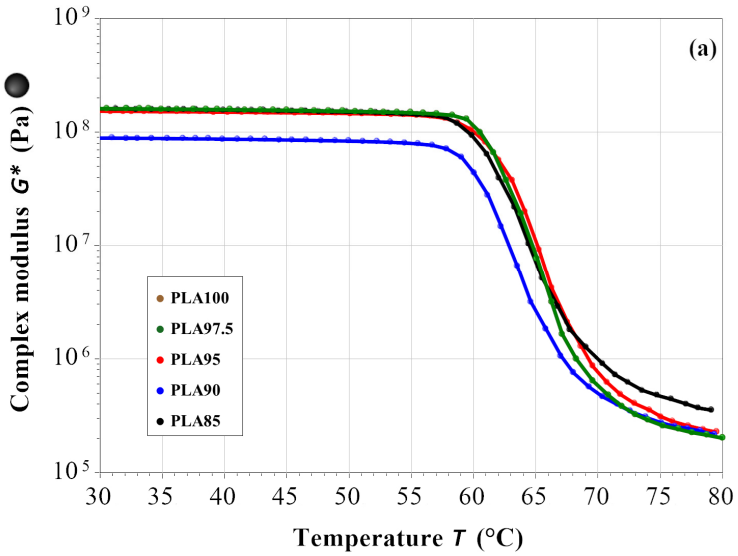

Figure 5. *Cont.*

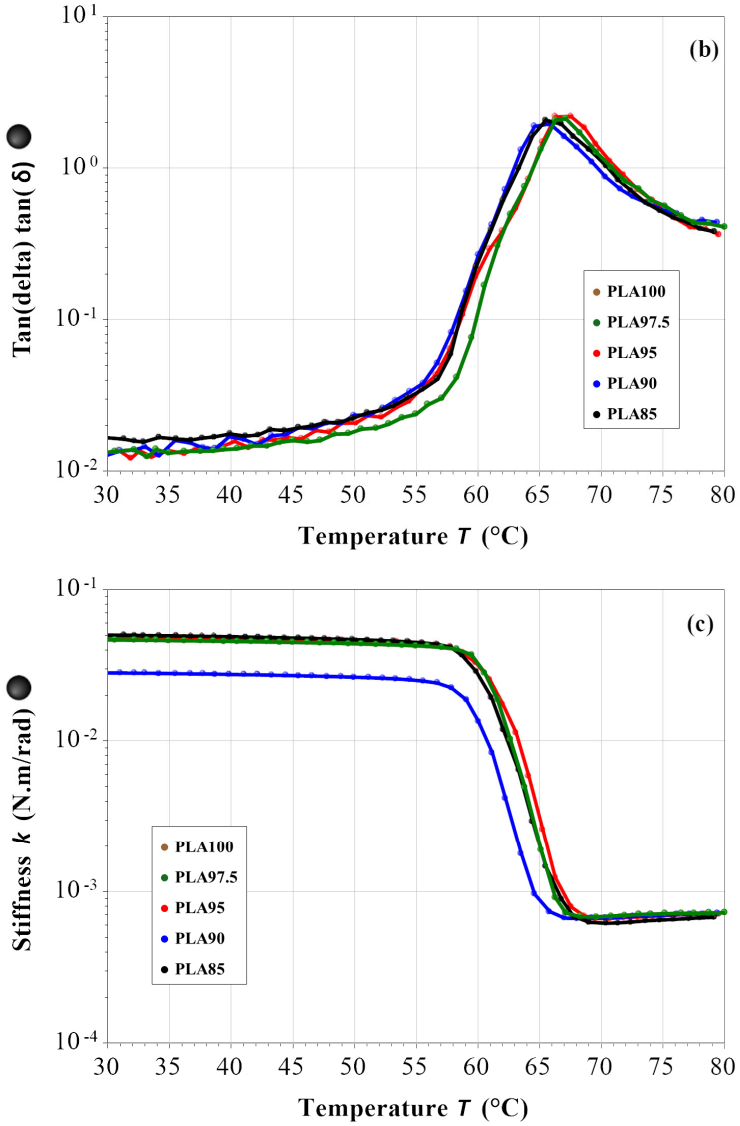

Figure 5. Temperature sweep results for the (**a**) complex modulus, (**b**) tan δ and (**c**) stiffness; for PLA85 in black, PLA90 in blue, PLA95 in red, PLA 97.5 in green and PLA100 in brown.

3.5.1. Surface Morphology

The pure PLA filament exhibited a smooth and homogeneous surface, as expected for an unfilled thermoplastic material [26]. With the addition of 2.5% chestnut burr (PLA97.5), slight surface roughness became visible. This effect became more pronounced at 10–15% filler content (PLA90 and PLA85). The increased roughness suggests a rise in exposed specific surface areas. A rougher surface can provide more area for bonding between layers. Similarly, in contexts requiring functional surface interactions (coatings, for instance), added texture may improve adherence through greater contact area. In addition, the surface texture associated with the natural filler may contribute to a more aesthetically appealing "natural" look, potentially valuable for sustainable design applications or biodegradable consumer products (Figure 6).

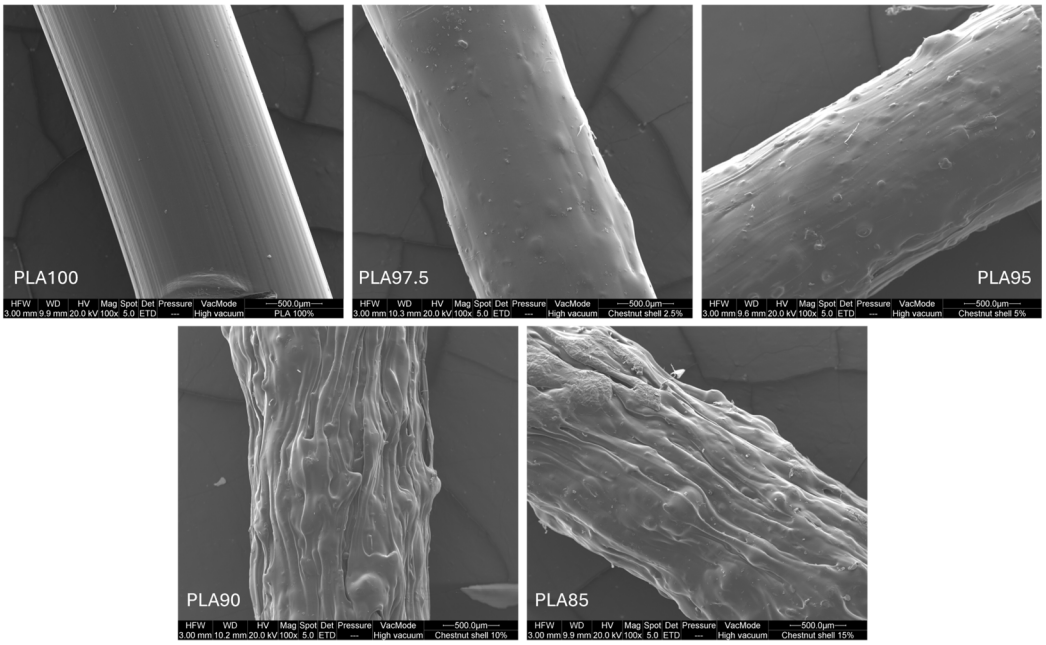

Figure 6. SEM micrographs of the external surface of extruded PLA/chestnut burr composite filaments at different filler loadings: PLA100, PLA97.5, PLA95, PLA90, and PLA85. Images were acquired at 100× magnification.

3.5.2. Cross-Sectional Morphology

Cross-sectional SEM images revealed that up to 5% chestnut burr content, the filler particles appeared evenly dispersed and well embedded within the PLA matrix, with no clearly visible signs of interfacial delamination. This indicates a satisfactory interfacial bonding between the filler and the polymer, which is crucial for mechanical stress transfer across the composite.

At higher filler contents (PLA90 and PLA85), the microstructure appeared more heterogeneous, with visible microvoids and slightly coarser dispersion. However, no macroscopic defects or cracks were observed, and the filler remained well integrated within the matrix. Importantly, no processing issues were detected during filament extrusion or FDM printing.

The chestnut burr powder was sieved below 200 µm, resulting in differently shaped particles with a broad size distribution typical of lignocellulosic residues. SEM analysis confirmed an homogeneous dispersion of these fine particles within the PLA matrix, supporting the material's good extrudability and printability.

These findings confirm that even at high filler contents, the material maintains satisfactory structural cohesion and processability. Although not directly measured in this study, such voids, when controlled, could potentially enhance material absorbency (Figure 7).

3.5.3. Functional Implications

The partial exposure of chestnut burr particles at the surface could favor the release of phenolic compounds, as hypothesized based on antioxidant activity results, described in the next paragraph. However, direct release or migration was not evaluated and would require further study [9]. This feature could make the material suitable for active packaging, where gradual release of natural antioxidants or antimicrobials is beneficial. Although gas barrier properties were not directly assessed in this work, the presence of lignocellulosic particles may influence permeability, as previously observed. For example, Camarena-Bononad et al. reported that PLA films containing Posidonia-derived lignocellulosic fibers exhibited reduced water vapor permeability, while their oxygen barrier performance improved

significantly [27]. From a thermal perspective, the distributed presence of finely divided filler particles could serve as nucleating agents, promoting more organized crystallization of the PLA during cooling [28]. DSC results, which show increased crystallinity with increasing filler content, support this hypothesis. Similar results were reported in the literature, showing that lignin-coated cellulose nanocrystals greatly increased the PLA composites' crystallisation rate and crystallinity [29]. Moreover, previous research shows how the inclusion of bamboo fibers in PBS promoted crystallization and crystallinity in the composites [30].

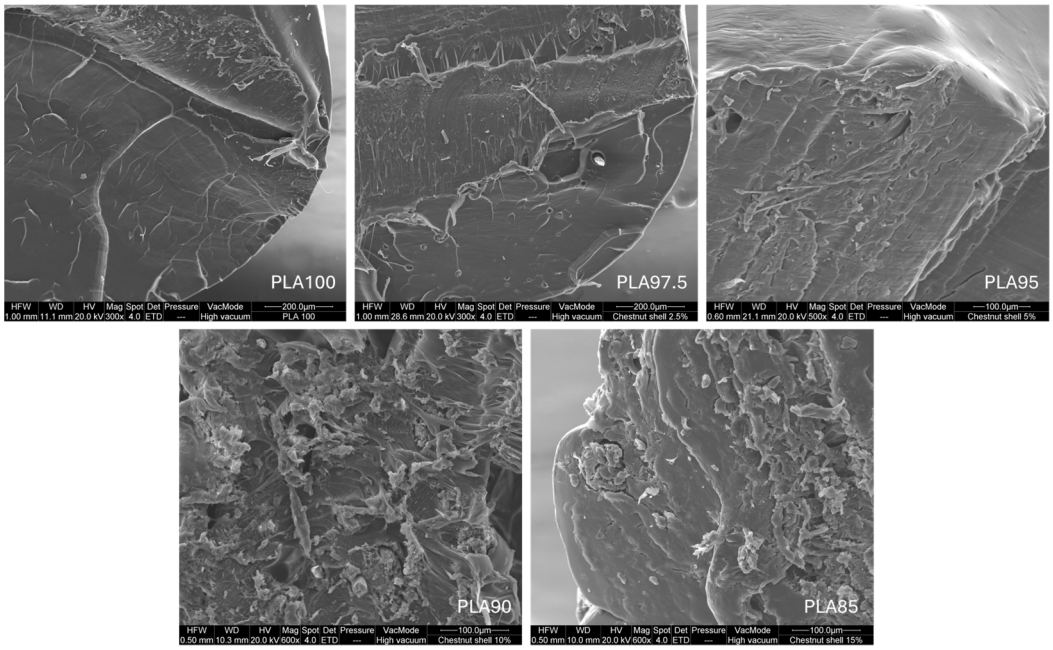

Figure 7. Cross-sectional SEM images of PLA/chestnut burr composite filaments with increasing filler content: PLA100, PLA97.5 (300×), PLA95 (500×), PLA90 and PLA85 (600×).

Last but not least, high-filler formulations may make it easier for water to seep into the material due to their increased surface roughness and microstructural discontinuities.

This could potentially enhance hydrolytic and microbial degradation under composting conditions, an effect that has been reported in the literature in PLA composites containing lignocellulosic fillers [31]. Beyond the microstructural considerations, evidence from the literature indicates that the incorporation of chestnut burr filler may influence the environmental degradability of the developed biocomposite. Previous studies have demonstrated that *Castanea sativa* residues, such as burrs, are rich in lignocellulosic and polysaccharidic fractions readily degraded under microbial conditions [32,33]. Costa-Trigo et al. highlighted the susceptibility of chestnut burr components, mainly hemicellulose, cellulose, and lignin, to hydrolysis and biological oxidation, further supporting their inherent biodegradability [34]. Moreover, studies on PLA-biomass composites have shown that the presence of natural fillers can accelerate polymer disintegration under composting conditions. For example, the addition of algal biomass to PLA has been reported to enhance water uptake and facilitate enzymatic hydrolysis of the polymer during thermophilic composting [35]. In addition, other studies have reported that lignocellulosic fillers generally promote microbial attachment and create diffusion pathways for moisture and oxygen, thereby increasing PLA biodegradation rates [36]. Considering these findings, together with the morphological features observed in this study, specifically, the formation of limited microvoids that could act as preferential points for water penetration, it is reasonable to hypothesize that the inclusion of chestnut burr may favor the biodegradability of the

PLA-based composite under suitable composting conditions. Although this aspect was not experimentally assessed in the present study, it will be addressed in future work aimed at quantitatively evaluating degradation kinetics according to standardized protocols such as ISO 14855 and ASTM D5338 [37,38].

3.6. Antioxidant Activity (DPPH, ABTS, FRAP and Folin–Ciocâlteu Assays)

Antioxidant activity was evaluated to verify whether the bioactive compounds remained stable during extrusion and 3D printing processes or were degraded by thermal treatment. The choice of carrying out the assays on PLA85, which contained the highest concentration of filler, was made to assess the maximum potential bioactivity imparted by the natural component, as lower filler contents were expected to yield proportionally reduced effects. The incorporation of chestnut burr at 15% markedly increased the antioxidant response of PLA in all the assays performed. Pure PLA showed only a minor background signal, whereas the biocomposite displayed higher radical-scavenging capacity and reducing/phenolic content. After FDM printing, the antioxidant activity was substantially preserved, indicating that the processing conditions did not degrade the bioactive constituents released from the filler.

Using the DPPH assay, the neat PLA extract exhibited 0.122 ± 0.012 mg Trolox equivalents per gram of filament (mg TE/g). PLA85 composite before printing reached 0.402 ± 0.004 mg TE/g, and this value further increased to 0.513 ± 0.004 mg TE/g after printing (n = 3). The differences between the composite (pre- and post-printing) and neat PLA, as well as the increase induced by printing, were statistically significant (both $p < 0.0001$ vs. PLA100). This progressive increase suggests different things: phenolic constituents embedded in the filler are efficiently extracted; the mild thermal history of FDM may promote additional release/exposure of antioxidant moieties without causing their degradation.

Consistent trends were observed in the ABTS/TEAC assay. Neat PLA displayed 0.82 ± 0.020 µmol TE/g, whereas the biocomposite yielded ~2.2-fold higher values (1.81 ± 0.01 and 1.80 ± 0.02 µmol TE/g before and after printing, respectively). The enhancement relative to neat PLA was significant (both $p < 0.0001$ vs. PLA100), while the difference between pre- and post-printing composites was negligible, confirming that the radical scavenging activity of the chestnut burr phenolics is retained after extrusion and during printing process.

The reducing power measured by FRAP increased from 0.348 ± 0.009 mg ascorbic acid equivalents per gram (mg AAE/g) in neat PLA to 0.703 ± 0.02 mg AAE/g in the composite before printing and 1.128 ± 0.034 mg AAE/g after printing ($p < 0.0001$ for PLA100 vs. pre and post-printing). Similarly, total phenolic content (Folin–Ciocâlteu) rose from 0.350 ± 0.013 mg gallic acid equivalents per gram (mg GAE/g) for PLA to 0.507 ± 0.017 mg GAE/g (pre-printing) and 0.691 ± 0.07 mg GAE/g (post-printing) ($p < 0.0001$ for both samples vs. PLA100). The concordant increase in FRAP and TPC values after printing indicates that additional phenolic/reducing species become accessible, likely due to partial disruption of filler particles or improved polymer–filler interfacial area during melt deposition. Results are summarized in Table 3. The four antioxidant assays yielded coherent and complementary results, reflecting a common underlying mechanism of action. In particular, the total phenolic content measured by the Folin–Ciocâlteu method correlated well with both the reducing power (FRAP assay) and the radical scavenging activity (DPPH and ABTS assays). Polyphenolic compounds are known to act as efficient electron and hydrogen donors, thereby enhancing both redox capacity and free-radical scavenging ability. Consequently, the higher polyphenol content introduced by the chestnut burr directly explains the consistent increase observed across all tests. All assays were performed on the same

extract batches under harmonized experimental conditions, and data were normalized to sample mass. The consistent agreement among methods therefore confirms the reliability of the experimental approach.

Table 3. Antioxidant activity of neat PLA (PLA100) and PLA containing 15 wt% chestnut burr before (PLA85) and after 3D printing (PLA85 post-printing). DPPH and TEAC are expressed as mg and μmol Trolox equivalents per gram of material, respectively; RSA% indicates the percentage of DPPH• or ABTS•+ radical quenching. TPC: total phenolic content (Folin–Ciocâlteu, mg gallic acid equivalents/g); Reducing Power: FRAP assay (mg ascorbic acid equivalents/g). Values are mean ± standard deviation (n = 3). All differences between composite samples and PLA100 are statistically significant ($p < 0.0001$) unless otherwise stated.

Sample	DPPH (mgTE/g)	RSA% DPPH	TEAC (μmol TE/g)	RSA% ABTS	TPC (mg GAE/g)	Reducing Power (mg AAE/g)
PLA100	0.122 ± 0.012	23.78 ± 2.06	0.82 ± 0.02	42.83 ± 0.96	0.350 ± 0.013	0.348 ± 0.009
PLA85	0.402 ± 0.004	71.52 ± 0.69	1.81 ± 0.01	90.87 ± 0.36	0.507 ± 0.017	0.703 ± 0.02
PLA85 post-printing	0.513 ± 0.004	90.6 ± 0.61	1.8 ± 0.02	90.64 ± 0.17	0.691 ± 0.07	1.128 ± 0.034

Overall, the chestnut burr acts as an effective natural antioxidant source for PLA, conferring radical scavenging, reducing and phenolic functionalities. The preservation, and amplification in some assays, of activity after 3D printing demonstrates the suitability of the biocomposite for additive manufacturing applications where intrinsic antioxidant properties are desirable and exploitable for applications like active packaging. While the antioxidant assays confirm that the antioxidant potential of the chestnut burr filler is preserved after extrusion and 3D printing, it is important to highlight that, firstly, these assays are indicative of general radical scavenging capacity and antioxidant capacity. They do not fully replicate the conditions of real-world applications such as contact with food surfaces or biological tissues. Therefore, complementary studies involving contact-based or surface-specific tests would be beneficial to further validate the practical effectiveness of the antioxidant properties in applied contexts [39].

Bianchi et al. reported a similar result, showing that following processing in a poly(1,4-butylene succinate) (PBS) matrix, phenolic extracts derived from industrial coffee residues maintained their antioxidant activity. This result is in line with our findings on PLA filled with chestnut burrs and demonstrates that some natural antioxidants can maintain their functional activity even after being subjected to heat processing like melt extrusion [40].

4. Conclusions

This study demonstrates the feasibility of producing PLA-based biocomposites incorporating chestnut burrs (*Castanea sativa*), an abundant lignocellulosic agro-industrial residue, as a multifunctional filler. Composite filaments with up to 15 wt% chestnut burr content were successfully prepared via melt extrusion and proved compatible with standard FDM 3D printing processes. Thorough chemical, thermal, mechanical, and morphological analyses verified that the PLA matrix's structural integrity and viscoelastic performance were not compromised by the incorporation of the natural filler. Notably, the filler acted as a nucleating agent promoting increased crystallinity and induced only minor reductions in thermal stability, remaining well within safe processing margins. The chestnut burr imparted the material functional activity in addition to its structural role. Antioxidant assays (DPPH, ABTS, FRAP, and Folin–Ciocâlteu) revealed a significant enhancement in radical-scavenging and reducing capacity, with these properties largely preserved, or

even increased, after 3D printing. This confirms that the bioactive compounds within the filler can withstand melt processing without degradation. Taken together, these findings highlight chestnut burrs as an effective dual-function filler that increases the biobased content of PLA while introducing antioxidant functionality. Based on these results, chestnut burrs show strong potential as biobased fillers for PLA, enabling the development of multipurpose composite materials suitable for active packaging applications. In this context, the material's intrinsic antioxidant functionality could help protect sensitive goods from oxidative degradation. This functional behavior, coupled with its fully biobased composition and FDM processability, highlights the material's suitability for sustainable packaging and other high-value applications where oxidative stability is desired.

Moreover, based on previous evidence on chestnut residues and PLA-biomass composites, the inclusion of the chestnut burr filler may enhance the biodegradability of the composite filaments. Future studies will verify this through standardized composting assays.

Finally, it should be emphasized that the 3D printing experiments in this work were designed for exploratory purposes to assess the processability and functional stability of the developed composite rather than to perform an exhaustive mechanical evaluation of printed objects. All formulations, including those containing 10 wt% and 15 wt% chestnut burr, were successfully printed under standard FDM conditions for PLA, confirming the overall printability and process reliability of the materials. At higher filler loadings, minor surface irregularities and microvoids were observed by SEM, but these did not compromise the extrusion or printing process. Further work will focus on assessing the 3D-printed parts in more detail and on optimizing the filler content for specific application requirements. This clarification explicitly defines the exploratory nature and scope of the present study, whose main objective was the development and characterization of a PLA/chestnut burr biocomposite.

Author Contributions: Conceptualization, T.O., S.P., M.G. and A.S.; methodology, T.O., S.P., M.S. and E.P.; validation, V.T., A.T. and A.V.; investigation, T.O., S.P. and M.S.; resources, A.S. and A.M.; data curation, T.O., S.P. and M.G.; writing—original draft preparation, T.O. and S.P.; writing—review and editing, T.O., S.P. and M.G.; visualization T.O. and S.P.; supervision, A.S., A.M., P.L. and M.G.; project administration, A.S.; funding acquisition, A.S. All authors have read and agreed to the published version of the manuscript.

Funding: Regione Toscana—CHEBAPACK Programma di Sviluppo Rurale 2014–2020—Misura 16.2—GAL FAR Maremma—Sostegno a progetti pilota e di cooperazione, CUP B67G22000090001; European Union—NextGenerationEU within the National Recovery and Resilience Plan (PNRR), Mission 4, Component 2, Investment 1.4—Project PNRR CN3 "mRNA"—Spoke 5—CUP B63C22000610006, and Investment 1.5—Creation and reinforcement of an "innovation ecosystem", construction of "leader territoriali R&S"—Project THE (Tuscan Health Ecosystem)—Spoke 4—Nanotechnologies for diagnosis and therapy—project code ECS00000017, CUP B63C22000680007.

Institutional Review Board Statement: Not applicable.

Informed Consent Statement: Not applicable.

Data Availability Statement: The original contributions presented in this study are included in the article. Further inquiries can be directed to the corresponding author.

Conflicts of Interest: Michela Geminiani and Annalisa Santucci were employed by the University of Siena and were co-founders of the university spin-off SienabioACTIVE. Author Annalisa Santucci was also affiliated with the company ARTES 4.0, a Competence Center for Industry 4.0 operating as a public-private consortium. ARTES 4.0 is a non-profit research and innovation organization, not a traditional for-profit company. The role of the company in this study is none. The remaining authors declare that the research was conducted in the absence of any commercial or financial rela-tionships that could be construed as a potential conflict of interest.

References

1. Atiwesh, G.; Mikhael, A.; Parrish, C.C.; Banoub, J.; Le, T.A.T. Environmental Impact of Bioplastic Use: A Review. *Heliyon* **2021**, *7*, e07918. [CrossRef] [PubMed]
2. Sangeetha, V.H.; Deka, H.; Varghese, T.O.; Nayak, S.K. State of the Art and Future Prospectives of Poly(Lactic Acid) Based Blends and Composites. *Polym. Compos.* **2018**, *39*, 81–101. [CrossRef]
3. Sherwani, S.F.K.; Zainudin, E.S.; Sapuan, S.M.; Leman, Z.; Khalina, A. Recent Development of Natural Fibers Reinforced Polylactic Acid Composites. *J. Res. Nanosci. Nanotechnol.* **2022**, *5*, 103–108. [CrossRef]
4. Venkatesh, G. Circular Bio-Economy—Paradigm for the Future: Systematic Review of Scientific Journal Publications from 2015 to 2021. *Circ. Econ. Sustain.* **2022**, *2*, 231–279. [CrossRef]
5. Trivedi, A.K.; Gupta, M.K.; Singh, H. PLA Based Biocomposites for Sustainable Products: A Review. *Adv. Ind. Eng. Polym. Res.* **2023**, *6*, 382–395. [CrossRef]
6. Çıtlacıfçı, H.; Kılıç Pekgözlü, A.; Gülsoy, S.K. Characterization of Chestnut Shell. *Bartın Univ. Int. J. Nat. Appl. Sci.* **2022**, *5*, 145–150. [CrossRef]
7. Frusciante, L.; Geminiani, M.; Olmastroni, T.; Mastroeni, P.; Trezza, A.; Salvini, L.; Lamponi, S.; Spiga, O.; Santucci, A. Repurposing *Castanea sativa* Spiny Burr By-Products Extract as a Potentially Effective Anti-Inflammatory Agent for Novel Future Biotechnological Applications. *Life* **2024**, *14*, 763. [CrossRef]
8. Trezza, A.; Barletta, R.; Geminiani, M.; Frusciante, L.; Olmastroni, T.; Sannio, F.; Docquier, J.D.; Santucci, A. Chestnut Burrs as Natural Source of Antimicrobial Bioactive Compounds: A Valorization of Agri-Food Waste. *Appl. Sci.* **2024**, *14*, 6552. [CrossRef]
9. Łopusiewicz, Ł.; Jędra, F.; Mizielińska, M. New Poly(lactic acid) Active Packaging Composite Films Incorporated with Fungal Melanin. *Polymers* **2018**, *10*, 386. [CrossRef]
10. Papadopoulou, E.L.; Paul, U.C.; Tran, T.N.; Suarato, G.; Ceseracciu, L.; Marras, S.; D'arcy, R.; Athanassiou, A. Sustainable Active Food Packaging from Poly(Lactic Acid) and Cocoa Bean Shells. *ACS Appl. Mater. Interfaces* **2019**, *11*, 31317–31327. [CrossRef]
11. Bhagia, S.; Bornani, K.; Agarwal, R.; Satlewal, A.; Ďurkovič, J.; Lagaňa, R.; Bhagia, M.; Yoo, C.G.; Zhao, X.; Kunc, V.; et al. Critical Review of FDM 3D Printing of PLA Biocomposites Filled with Biomass Resources, Characterization, Biodegradability, Upcycling and Opportunities for Biorefineries. *Appl. Mater. Today* **2021**, *24*, 101078. [CrossRef]
12. Zhang, G.; Li, J.; Li, J.; Zhou, X.; Xie, J.; Wang, A. Selective Laser Melting Molding of Individualized Femur Implant: Design, Process, Optimization. *J. Bionic. Eng.* **2021**, *18*, 128–137. [CrossRef]
13. Alothman, O.Y.; Awad, S.; Siakeng, R.; Khalaf, E.M.; Fouad, H.; Abd El-salam, N.M.; Ahmed, F.; Jawaid, M. Fabrication and Characterization of Polylactic Acid/Natural Fiber Extruded Composites. *Polym. Eng. Sci.* **2023**, *63*, 1234–1245. [CrossRef]
14. Lendvai, L. Lignocellulosic Agro-Residue/Polylactic Acid (PLA) Biocomposites: Rapeseed Straw as a Sustainable Filler. *Clean. Mater.* **2023**, *9*, 100196. [CrossRef]
15. Pepi, S.; Talarico, L.; Leone, G.; Bonechi, C.; Consumi, M.; Boldrini, A.; Lauro, A.; Magnani, A.; Rossi, C. Effect of Mild Conditions on PVA-Based Theta Gel Preparation: Thermal and Rheological Characterization. *Int. J. Mol. Sci.* **2024**, *25*, 12039. [CrossRef]
16. Muccilli, V.; Maccarronello, A.E.; Rasoanandrasana, C.; Cardullo, N.; de Luna, M.S.; Pittalà, M.G.G.; Riccobene, P.M.; Carroccio, S.C.; Scamporrino, A.A. Green3: A Green Extraction of Green Additives for Green Plastics. *Heliyon* **2024**, *10*, e24469. [CrossRef]
17. Song, F.L.; Gan, R.Y.; Zhang, Y.; Xiao, Q.; Kuang, L.; Li, H. Bin Total Phenolic Contents and Antioxidant Capacities of Selected Chinese Medicinal Plants. *Int. J. Mol. Sci.* **2010**, *11*, 2362–2372. [CrossRef]
18. Jayaprakasha, G.K.; Singh, R.P.; Sakariah, K.K. Antioxidant Activity of Grape Seed (*Vitis vinifera*) Extracts on Peroxidation Models in Vitro. *Food Chem.* **2001**, *73*, 285–290. [CrossRef]
19. Frusciante, L.; Geminiani, M.; Shabab, B.; Olmastroni, T.; Scavello, G.; Rossi, M.; Mastroeni, P.; Nyong'a, C.N.; Salvini, L.; Lamponi, S.; et al. Exploring the Antioxidant and Anti-Inflammatory Potential of Saffron (Crocus Sativus) Tepals Extract within the Circular Bioeconomy. *Antioxidants* **2024**, *13*, 1082. [CrossRef]
20. Choksi, N.; Desai, H. Synthesis of Biodegradable Polylactic Acid Polymer By Using Lactic Acid Monomer. *Int. J. Appl. Chem.* **2017**, *13*, 377–384.
21. Narlıoğlu, N.; Salan, T.; Alma, M.H. Properties of 3D-Printed Wood Sawdust-Reinforced PLA Composites. *BioResources* **2021**, *16*, 5467–5480. [CrossRef]
22. Leone, G.; Pepi, S.; Consumi, M.; Lamponi, S.; Fragai, M.; Martinucci, M.; Baldoneschi, V.; Francesconi, O.; Nativi, C.; Magnani, A. Sodium Hyaluronate-g-2-((N-(6-Aminohexyl)-4-Methoxyphenyl)Sulfonamido)-N-Hydroxyacetamide with Enhanced Affinity towards MMP12 Catalytic Domain to Be Used as Visco-Supplement with Increased Degradation Resistance. *Carbohydr. Polym.* **2021**, *271*, 118452. [CrossRef] [PubMed]
23. Patti, A.; Acierno, S.; Cicala, G.; Zarrelli, M.; Acierno, D. The Understanding the Processing Window of Virgin and Recycled Bio-Based Filaments for 3D Printing Applications. *Macromol. Symp.* **2022**, *405*, 2100291. [CrossRef]
24. Tábi, T.; Sajó, I.E.; Szabó, F.; Luyt, A.S.; Kovács, J.G. Crystalline Structure of Annealed Polylactic Acid and Its Relation to Processing. *Express Polym. Lett.* **2010**, *4*, 659–668. [CrossRef]

25. Song, L.; Li, Y.; Meng, X.; Wang, T.; Shi, Y.; Wang, Y.; Shi, S.; Liu, L. Crystallization, Structure and Significantly Improved Mechanical Properties of PLA/PPC Blends Compatibilized with PLA-PPC Copolymers Produced by Reactions Initiated with TBT or TDI. *Polymers* **2021**, *13*, 3245. [CrossRef]
26. Hui, I.; Pasquier, E.; Solberg, A.; Agrenius, K.; Håkansson, J.; Chinga-Carrasco, G. Biocomposites Containing Poly(Lactic Acid) and Chitosan for 3D Printing—Assessment of Mechanical, Antibacterial and in Vitro Biodegradability Properties. *J. Mech. Behav. Biomed. Mater.* **2023**, *147*, 106136. [CrossRef]
27. Camarena-Bononad, P.; Freitas, P.A.V.; González-Martínez, C.; Chiralt, A.; Vargas, M. Influence of the Purification Degree of Cellulose from Posidonia Oceanica on the Properties of Cellulose-PLA Composites. *Polysaccharides* **2024**, *5*, 807–822. [CrossRef]
28. Yang, J.Y.; Kim, D.K.; Han, W.; Park, J.Y.; Kim, K.W.; Kim, B.J. Effect of Nucleating Agents Addition on Thermal and Mechanical Properties of Natural Fiber-Reinforced Polylactic Acid Composites. *Polymers* **2022**, *14*, 4263. [CrossRef]
29. Gupta, A.; Simmons, W.; Schueneman, G.T.; Mintz, E.A. Lignin-Coated Cellulose Nanocrystals as Promising Nucleating Agent for Poly(Lactic Acid). *J. Therm. Anal. Calorim.* **2016**, *126*, 1243–1251. [CrossRef]
30. Thumsorn, S.; Srisawat, N.; On, J.W.; Pivsa-Art, S.; Hamada, H. Crystallization Kinetics and Thermal Resistance of Bamboo Fiber Reinforced Biodegradable Polymer Composites. In *AIP Conference Proceedings*; American Institute of Physics Inc.: College Park, MD, USA, 2014; Volume 1593, pp. 316–319.
31. Szczepanik, E.; Szatkowski, P.; Molik, E.; Pielichowska, K. The Effect of Natural Plant and Animal Fibres on PLA Composites Degradation Process. *Appl. Sci.* **2024**, *14*, 5600. [CrossRef]
32. Ventorino, V.; Parillo, R.; Testa, A.; Viscardi, S.; Espresso, F.; Pepe, O. Chestnut Green Waste Composting for Sustainable Forest Management: Microbiota Dynamics and Impact on Plant Disease Control. *J. Environ. Manag.* **2016**, *166*, 168–177. [CrossRef] [PubMed]
33. Ventorino, V.; Parillo, R.; Testa, A.; Aliberti, A.; Pepe, O. Chestnut Biomass Biodegradation for Sustainable Agriculture. *BioResources* **2013**, *8*, 4647–4658. [CrossRef]
34. Costa-Trigo, I.; Otero-Penedo, P.; Outeiriño, D.; Paz, A.; Domínguez, J.M. Valorization of Chestnut (*Castanea sativa*) Residues: Characterization of Different Materials and Optimization of the Acid-Hydrolysis of Chestnut Burrs for the Elaboration of Culture Broths. *Waste Manag.* **2019**, *87*, 472–484. [CrossRef]
35. Kalita, N.K.; Damare, N.A.; Hazarika, D.; Bhagabati, P.; Kalamdhad, A.; Katiyar, V. Biodegradation and Characterization Study of Compostable PLA Bioplastic Containing Algae Biomass as Potential Degradation Accelerator. *Environ. Chall.* **2021**, *3*, 100067. [CrossRef]
36. Cruz Fabian, D.R.; Durpekova, S.; Dusankova, M.; Cisar, J.; Drohsler, P.; Elich, O.; Borkova, M.; Cechmankova, J.; Sedlarik, V. Renewable Poly(Lactic Acid)Lignocellulose Biocomposites for the Enhancement of the Water Retention Capacity of the Soil. *Polymers* **2023**, *15*, 2243. [CrossRef]
37. *ISO 14855-1:2012*; Determination of the Ultimate Aerobic Biodegradability of Plastic Materials Under Controlled Composting Conditions—Method by Analysis of Evolved Carbon Dioxide-Part 1: General Method. International Organization for Standardization: Geneva, Switzerland, 2012.
38. *ASTM D5338-15*; Standard Test Method for Determining Aerobic Biodegradation of Plastic Materials Under Controlled Composting Conditions. ASTM International: West Conshohocken, PA, USA, 2015.
39. Sadeer, N.B.; Montesano, D.; Albrizio, S.; Zengin, G.; Mahomoodally, M.F. The Versatility of Antioxidant Assays in Food Science and Safety-Chemistry, Applications, Strengths, and Limitations. *Antioxidants* **2020**, *9*, 709. [CrossRef]
40. Bianchi, S.; Marchese, P.; Vannini, M.; Sisti, L.; Tassoni, A.; Ferri, M.; Mallegni, N.; Cinelli, P.; Celli, A. Evaluation of the Activity of Natural Phenolic Antioxidants, Extracted from Industrial Coffee Residues, on the Stability of Poly(1,4-Butylene Succinate) Formulations. *J. Appl. Polym. Sci.* **2023**, *140*, e53878. [CrossRef]

Disclaimer/Publisher's Note: The statements, opinions and data contained in all publications are solely those of the individual author(s) and contributor(s) and not of MDPI and/or the editor(s). MDPI and/or the editor(s) disclaim responsibility for any injury to people or property resulting from any ideas, methods, instructions or products referred to in the content.